

A prospective comparison of a modified miniaturised hand-held epifluorescence microscope and touch imprint cytology for evaluation of axillary sentinel lymph nodes intraoperatively in breast cancer patients

Jia-jian Chen¹  | Bao-hua Yu² | Ti-jing Shen³ | Ying Wang⁴ | Fei Ren² | Li-rui Yang² | Yuan Dong⁵ | Ming-jie Zheng⁶ | Shuang Hao¹ | Wen-tao Yang² | Jiong Wu^{1,7}

¹Department of Breast Surgery, Key Laboratory of Breast Cancer in Shanghai, Fudan University Shanghai Cancer Center, Shanghai, China

²Department of Pathology, Fudan University Shanghai Cancer Center, Shanghai, China

³Baoshan People's Hospital, Baoshan, China

⁴Department of Thyroid and Breast Surgery, Affiliated Hospital of Yangzhou University, Yangzhou, China

⁵Department of Breast Surgery, The First Affiliated Hospital of Kunming Medical University, Kunming, China

⁶Department of Breast Surgery, The First Affiliated Hospital with Nanjing Medical University, Nanjing, China

⁷Collaborative Innovation Center for Cancer Medicine, Shanghai, China

Correspondence

Jiong Wu and Wen-tao Yang, No. 270 Dong An Road, Shanghai, China.
Email: wujiong1122@vip.sina.com and yangwt2000@163.com

Abstract

Background: The management of axillary lymph nodes in early-stage breast cancer patients has changed considerably, with the primary focus shifting from the examination of sentinel lymph nodes (SLNs) to toward the detection of all macro-metastases. However, current methods, such as touch imprint cytology (TIC) and frozen sections, are inadequate for clinical needs. To address this issue, we proposed a novel miniaturised epifluorescence widefield microscope (MEW-M) to assess SLN status intraoperatively for improved diagnostic efficiency.

Methods: A prospective, side-by-side comparison of intraoperative SLN evaluation between MEW-M and TIC was performed.

Results: A total of 73 patients with 319 SLNs consecutive enrolled in this study. MEW-M showed significantly superior image quality compared to TIC (median score 3.1 vs 2.1, $p < 0.0001$) and had a shorter time to issue results (10.3 vs 19.4 min, $p < 0.0001$). Likelihood ratio analysis illustrated that the positive likelihood ratio value of MEW-M compared with TIC was infinitely great vs 52.37 (95% CI, 21.96-124.90) in model 1 (classifying results into negative/positive), infinitely great vs 52.37 (95% CI, 21.96-124.90) in model 2 (classifying results into macro-metastasis/others, and TIC results followed the same classification as model 1), respectively. Similarly, the negative likelihood ratio values of MEW-M compared with TIC were 0.055 (95% CI, 0.018-0.160) and 0.074 (95% CI, 0.029-0.190) in model 1; and 0.019 (95% CI, 0.003-0.130) vs 0.020 (95% CI, 0.003-0.140) in model 2, respectively.

Conclusions: MEW-M is a promising technique that can be utilised to provide a rapid and accurate intraoperative assessment of SLN in a clinical setting to help improve decision-making in axillary surgery.

KEYWORDS

breast cancer, lymphatic metastasis, microscopy, sentinel lymph node



1 | INTRODUCTION

Over the last few decades, management of the axilla in early-stage breast cancer has focused on de-escalation surgery,^{1,2} with the aim of improving patients' quality of life while ensuring their survival.² Sentinel lymph node biopsy (SLNB) is the best practice in terms of the standard of care for most clinical node-negative patients,^{3,4} since it has a lower morbidity than routine lymphadenectomy⁵ and similarly avoids unnecessary reoperation due to undetected sentinel lymph node metastases.⁶

Intraoperative evaluation of sentinel lymph node (SLN) metastasis status is mainly performed using touch imprint cytology (TIC) and frozen sections (FS).^{7,8} However, most centres in the UK still rely solely on traditional histopathological examination, which may necessitate delayed axillary clearance in up to 25% of patients.⁹ The reason for this is that the current intraoperative detection methods are not well suited to meet clinical needs.¹⁰ FS requires time and is a labour-intensive process, making it unsuitable for real-time decision-making.^{11,12} By contrast, TIC is considered the best available method for intraoperative SLN evaluation,¹³ with the advantages of there being minimal tissue preparation requirements and no need for expensive equipment, and the fact that it is a faster alternative to FS that is equally accurate.^{7-9,14,15} Nevertheless, a higher false-positive rate has been recorded, resulting in unnecessary axillary lymph node dissection in 15.5% of cases, according to the latest guidelines.⁶ This phenomenon could be due to its lower ability to identify metastatic lesions that are less than 2 mm in diameter.^{6,16}

To address this issue, we conducted a prospective side-by-side comparison of the intraoperative performance of SLNs between a novel non-destructive cell microscopic (MEW-M) technique and TIC to demonstrate the feasibility and diagnostic efficiency of MEW-M in the intraoperative assessment of human breast cancer SLN status.

2 | MATERIALS AND METHODS

2.1 | Patients and design

This prospective ex-vivo diagnostic test was conducted at the Fudan University Shanghai Cancer Center (FUSCC) and was approved by the local Institutional Ethics Committee. Diagnostic results from different techniques were obtained using a blinded design, and all patients provided written informed consent. Seventy-three women with early breast cancer treated with SLNB were consecutively enrolled in this study between September 2022 and January 2023. Patients younger than 18 years of age were excluded from this study. Additional exclusion criteria were T3/T4 tumour, absence of MEW-M, or touch imprint cytology interpretation. A mutually blinded design was applied to the interpretation of the MEW-M and TIC results.

2.2 | Miniaturised epifluorescence widefield microscope system

MEW-M (MDS-1000; Dendrite Precision Medical Ltd.) is a modified real-time miniaturised epifluorescence microscope that generates a pseudo-histological image. It is an iterative model from DiveScope (Micro Control Instruments)¹⁷ with an anti-shake performance. The MEW-M system consists of an image acquisition system, light emitting diode (LED) light source, camera readout, and monitor (a diagram of the MEW-M architecture is presented in Figure S1A). The LED laser source transmits light to the camera for readout via a fibre optic coupler and a scanning delivery fibre. The blue laser light (475 nm wavelength) focuses the sample at a depth of 50 µm with a field of view (FOV) of 0.5 mm and a zoom range of 500× to 1280×. To allow for hand-held operation, the lens is 14 cm in length and 3 mm in diameter. Additionally, the optical image stabilisation (OIS) design, coupled with a resolution of up to 0.5 µm and 60 frames/s, enables high-resolution real-time imaging. A 4 mm diameter sterile sheath is also present, protecting the lens from contamination and maintaining a consistent distance between the tip of the zoom lens and the tissue surface for optimal imaging quality. Probing tissue requires the use of sodium fluorescein and methylene blue (Patent ID: CN113358614A), which work through dyeing mechanisms. (The staining procedure is shown in Figure S1B.) Sodium fluorescein is an active fluorescent dye that uses an aqueous solution to mark the outlines of cells, enhancing their visualisation. In contrast, methylene blue, an alkaline fluorescent dye, stains the nucleus of cells, increasing the contrast between the tumour and surrounding tissue due to the tumour's abundant deoxyribonucleic acid.¹⁸ The image acquisition system receives and processes the emitted green light (530 nm wavelength) from stained tissue and displays it on the monitor as an image (1920×1080 pixels) with two colour sets to choose from: black and white, or black and green.

2.3 | Touch imprint cytology sample processing and diagnosis

The surgeon performed the standard blue-dye method for SLN identification¹⁹; 2 mL of methylene blue dye was injected into the upper outer quadrant of the breast region after the induction of anaesthesia. SLNs were immediately harvested and sent to the pathology department for intraoperative diagnosis. SLNs with a diameter of less than 4 mm were bisected, whereas the remainder were serially sectioned (2–3 mm each) along the short axis by the cytologist on the grossing bench. Each cut surface of the same lymph node is touched to the same slide. Haematoxylin-eosin (H&E) staining was used for the TIC samples, which were then evaluated by a dedicated cytologist (Ren F) who assigned each case to one of two possible diagnostic categories: SLN-negative or SLN-positive (contains suspicious cell clusters) for metastatic disease. If any TIC was positive for metastatic disease, an immediate axillary lymph node dissection (ALND) was performed.

2.4 | Miniaturised epifluorescence widefield microscope image acquisition and interpretation

A junior pathologist (Yang LR) performed all procedures in the cytology lab and was trained for an hour in imaging acquisition and diagnosis. We streamlined the processes of sample preparation and interpretation to expedite them. Figure 1 shows the key points of the assembly line operation. When the specimen contained more than one lymph node, the sections were stained at the same time. Furthermore, the 'scan and interpret' principle was applied, wherein the size of metastatic foci was estimated by superimposing the microscopic FOV (each FOV is 0.5 mm in diameter). Lesions exceeding or equal to 2 mm in diameter were labelled as macro-metastases, those less than 0.2 mm as isolated tumour cells, and the rest as micro-metastases.²⁰ The MEW-M image acquisition and interpretation was carried out as follows: (1) 0.2% sodium fluorescein and 1% methylene blue solution were prepared by diluting 0.9% sodium chloride; (2) the most suspicious slice (characterised by greyish-white spots) of each lymph node was selected; if it was not possible to identify the most suspicious slice, the lymph node section with the largest diameter line was selected; (3) the slice was sprayed with diluted sodium fluorescein solution for 1.5 min, then washed with physiological saline; (4) the slice was sprayed with diluted methylene blue solution for 30s, then washed with a salt solution; (5) interpreting the images on the monitor while scanning, the pathological status of the SLNs was classified as negative (no carcinoma cells), lesions less than 2 mm, or macro-metastases (larger than 2 mm metastasis). Two images of the metastatic area in the positive group and each image of the cortical and medullary areas in the negative group were captured and saved, and the interpretation results were recorded.

The diagnostic comparison between TIC and MEW-M was conducted in a double-blind manner. The patients' information is publicly available. Routine histological examination was conducted as the gold standard, with each slice fixed in formalin and reviewed by a senior pathologist who was blinded to the MEW-M results. In

addition, the time taken from the sampling to the reporting of results was calculated for both MEW-M and TIC. Figure 2 shows the workflow chart.

2.5 | Image quality score

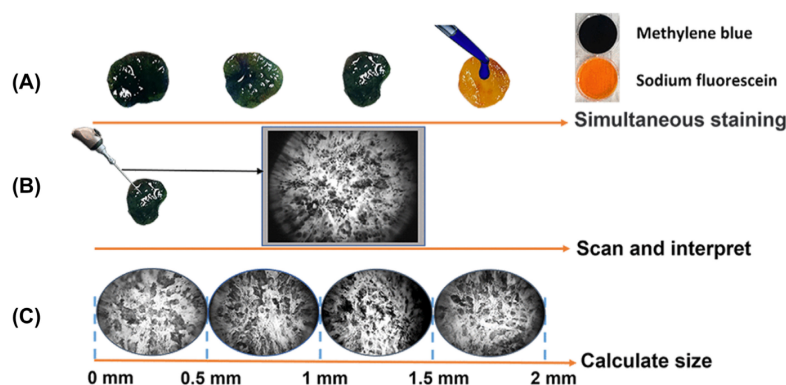
To assess the difficulty of interpretation of images obtained using MEW-M and TIC, an independent senior pathologist (Yu BH) evaluated the images, determining whether the images clearly showed the presence or absence of lymph node metastatic carcinoma based on staining clarity and the ability to recognise relevant features. Images were scored 4 if both indicators were optimal, 3 if one was suboptimal, 2 if both were general, and 1 if one was poor. The pathologist was pre-familiarised with 20 images of each technique before scoring.

2.6 | Statistical analysis

All statistical analyses were conducted using Medcalc statistical software (V19.0.4). The minimum sample size calculation was performed using Negida et al's methods.²¹ $N1$ was calculated $Z^2 \times \text{sensitivity} (1 - \text{sensitivity}) / W^2 / P$, and $N2$ was calculated $Z^2 \times \text{specificity} (1 - \text{specificity}) / W^2 / (1 - P)$. Z , the normal distribution value, was set to 1.96 to correspond with a 95% confidence interval, while W , the maximum acceptable width of the 95% confidence interval, was set to 10%. The sensitivity and specificity were both set at 0.9, while the positive event rate was set at 0.15. The negative event rate was set at 0.2. Finally, the minimum sample size for negative events ($N1$) was 231, and the minimum sample size for positive events ($N2$) was 41.

The permanent histopathology report was used as the gold standard for evaluating the accuracy of the TIC and MEW-M results. Statistical tests were two-sided and considered significant if $p < 0.05$. A paired samples t -test was performed to compare continuous variables. The diagnostic efficiency of the two methods was compared

FIGURE 1 Key points of assembly line operation. (A) Sections of multiple lymph nodes were stained simultaneously, first with fluorescein sodium and then with methylene blue. (B) While the lymph nodes are scanned, interpretation is performed using the monitor at the same time. (C) Lesion size was calculated by superimposing the microscopic field of view



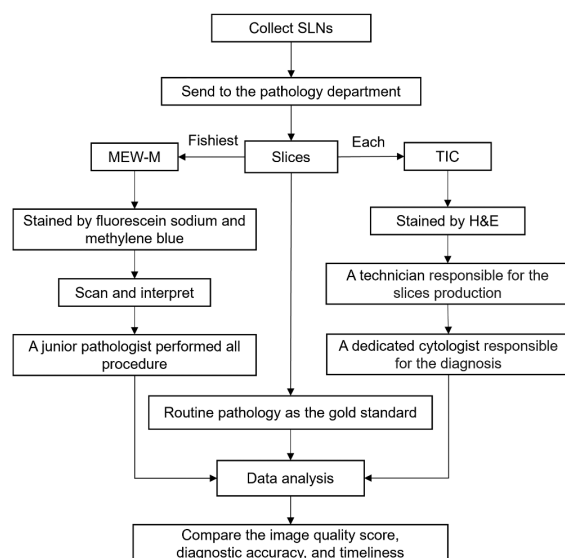


FIGURE 2 Workflow chart. H&E, hematoxylin-eosin; MEW-M, miniaturised epifluorescence widefield microscope; SLN, sentinel lymph node; TIC, touch imprint cytology.

using sensitivity, specificity, area under the receiver operating characteristic curve (AUC), positive likelihood ratio (PLR) and negative likelihood ratio (NLR).

3 | RESULTS

3.1 | Patient characteristics and final pathological diagnosis of SLNs

In this study, 73 female patients aged 31-74 years (mean age: 52.5 years) with early breast cancer (9 cases of ductal carcinoma in situ (DCIS), 66 of invasive ductal carcinomas, and 1 of invasive lobular carcinoma) underwent axillary surgery, yielding a total of 319 SLNs with a mean of 4.1 (range: 1-8) SLNs per axilla without missing data. Of these, ALND was performed in 35.6% of cases. Permanent pathology examination revealed 264 SLNs to be negative for metastatic tumour, 52 SLNs with macro-metastasis, and 3 SLNs with micro-metastasis (see Table S1).

3.2 | Hallmarks of SLNs in MEW-M and TIC images

Histological structure and cell pleomorphism were critical determinants in the pathology assessments using MEW-M and TIC. Figure 3 and Video S1 show how this new technology allows the clear and continuous display of lymph node structure, with an adenoid feature in the positive group, while the TIC images show reduced cell amounts and blurred tissue structure (Figure 3), which may make diagnosis more difficult.

3.3 | Image quality scores of MEW-M and TIC

A total of 319 MEW-M and 319 TIC images were evaluated from 319 SLNs. Figure 4 shows that the median MEW-M image quality score was 3.1, with 30% scoring 4, 50% scoring 3, and the remainder scoring 2. Conversely, the median TIC image quality score was 2.1, with 20% scoring 3, 50% scoring 2, and the remainder scoring 1.

3.4 | Comparison of the diagnostic performance between MEW-M and TIC

Interpretation results are classified into two categories, negative or positive, based on whether lymph nodes have metastasis, macro-metastasis, and others according to the recommended classification of early breast cancer axillary management guidelines.^{3,4,22} Figure 5 and Tables S2 and S3 present comparisons of the diagnostic performance of MEW-M and TIC.

3.5 | Model 1

Table S2 shows that the number of false negatives and false positives for TIC and MEW-M were 3 and 4, and 3 and 0, respectively. The detection rates of micro-metastasis were 0 (0/3) and 33.3% (1/3) for TIC and MEW-M, respectively. Receiver operating curve (ROC) analysis showed that the AUC value of MEW-M is slightly higher than that of TIC ($0.973 > 0.954$, $p = 0.258$), though this result was not statistically significant. The sensitivity, specificity, PLR, and NLR values for the identification of tumour deposits in SLNs using TIC were 92.7% (95% CI, 82.4%-98.0%), 98.1% (95% CI, 95.6%-99.4%), 48.96 (95% CI, 20.48-117.02), and 0.074 (95% CI, 0.029-0.190), respectively. By contrast, the sensitivity, specificity, PLR, and NLR values for MEW-M were 94.6% (95% CI, 84.9%-98.9%), 100.0% (95% CI, 98.6%-100.0%), infinitely great, and 0.055 (95% CI, 0.018-0.160), respectively (for ROC performance, see in Figure 5; Table S3 shows the diagnostic performance of MEW-M and TIC).

3.6 | Model 2

We compared the performance of MEW-M and TIC in the diagnosis of micro-metastases; three positive cases were converted to negative if the positive result was defined as a lesion larger than 2 mm. Our results showed excellent agreement between MEW-M and H&E (98.1%, 51/55). The results of the comparison between MEW-M and TIC are as follows: 0.990 (95% CI, 0.972-0.998) vs 0.981 (95% CI, 0.959-0.993) for AUC, $p = 0.514$; 98.08% (95% CI, 89.7%-100.0%) vs 98.08% (95% CI, 89.7%-100.0%) for sensitivity; 100.0% (95% CI, 98.6%-100.0%) vs 98.13% (95% CI, 95.7%-99.4%) for specificity; infinitely great vs 52.37 (95% CI, 21.96-124.90) for PLR; and 0.019 (95% CI, 0.003-0.130) vs 0.020 (95% CI, 0.003-0.140) for NLR (see Figure 5 and Table S3 for details).

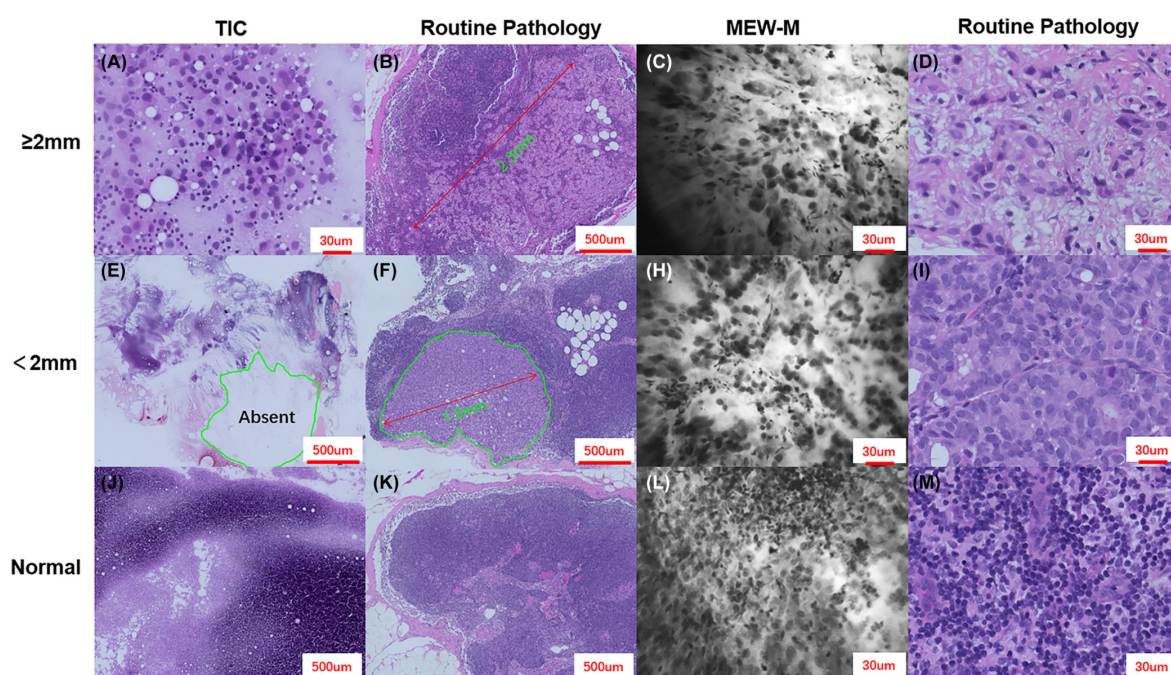
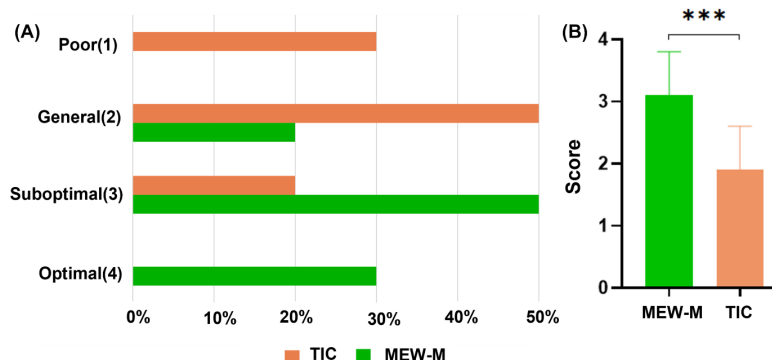


FIGURE 3 Comparison of images from three techniques. The images shown in (A–D), (E, F, H, I) and (J–M) show macro-metastases, micro-metastases and normal lymph nodes, respectively. TIC images are shown in (A, E, J), with corresponding paraffin pathology images in (B, F, K). MEW-M images are shown in (C, H, L), with corresponding conventional paraffin pathology images in (D, I, M). The TIC images show lower cell amounts, blurred tissue structures and uneven cell layers, resulting in staining that is too deep or too light. The image in (E) shows a complete loss of micro-metastases. The field of view of the MEW-M lens was fixed at $0.5 \times 0.5\text{ mm}$. The positive group (C, H) clearly shows a lymph node structure with adenoid features and abnormal nuclei. The negative group (L) shows an intact lymph node structure consisting of small round lymphocytes. Routine pathology was used as the gold standard, and digital slides could be measured visually on the software to measure lesion size. MEW-M, miniaturised epifluorescence widefield microscope; TIC, touch imprint cytology.

FIGURE 4 Image quality scores for MEW-M and TIC. (A) distribution of TIC and MEW-M image quality scores. (B) Median image score of TIC and MEW-M (***, $p < 0.001$). MEW-M, miniaturised epifluorescence widefield microscope; TIC, touch imprint cytology.



3.7 | Time-efficiency comparison between TIC and MEW-M

Complete timing data for both TIC and MEW-M were collected for 73 patients, with 78 timed examinations. Analyses of these data indicated that significantly less time was needed for MEW-M than for TIC. The median time for MEW-M was 10.3 min (range: 4–20 min) and for TIC was 19.4 min (range: 10–31 min). Generally, the MEW-M feedback was obtained within 4 min and the TIC feedback within

10 min for patients with only 1 SLN, plus approximately 2.3 minutes (MEW-M) and 3 min (TIC) for each additional node. Figure 6 shows the turnaround times for MEW-M and TIC.

4 | DISCUSSION

Surgical management of the axilla in early breast cancer has changed considerably, especially with regard to the indication of

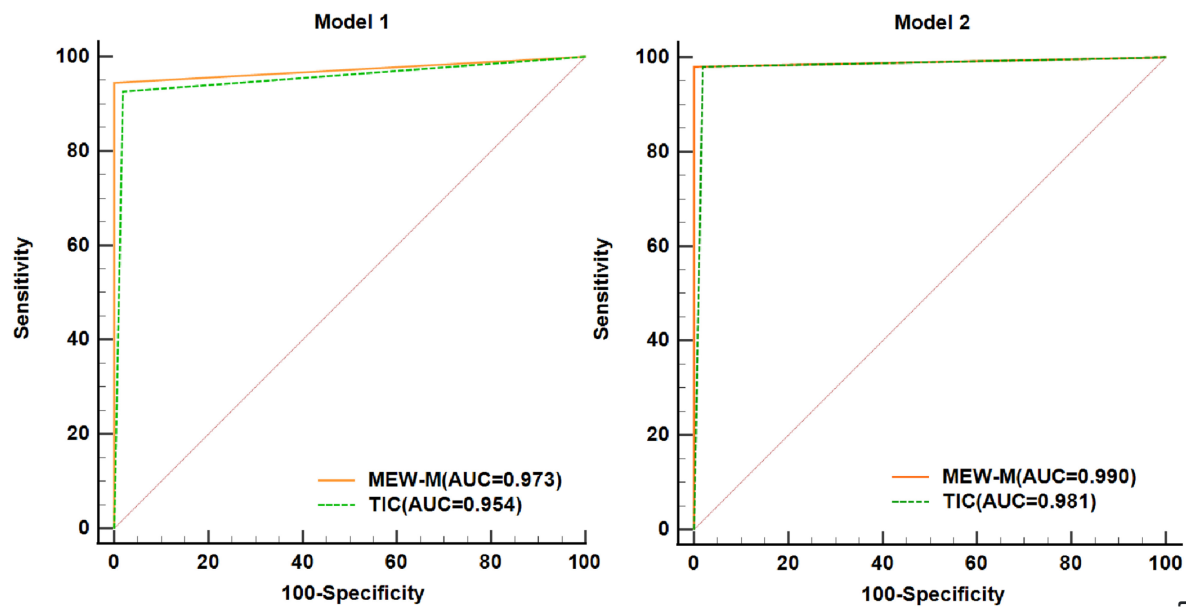


FIGURE 5 Receiver operating characteristic curves of the performance of two methods in assessing nodal status. AUC, area under the receiver operating characteristic curve.

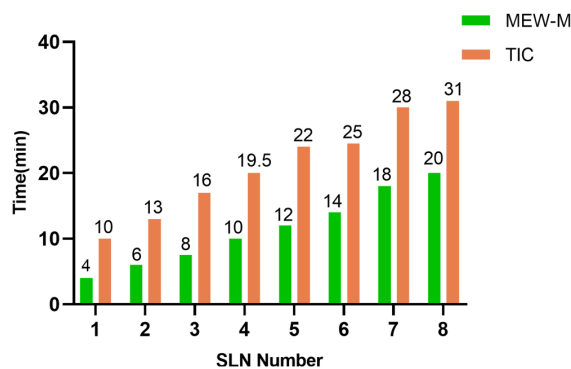


FIGURE 6 Comparison of the turnaround time between TIC and MEW-M. MEW-M, miniaturised epifluorescence widefield microscope; TIC, touch imprint cytology.

supplementary ALND.^{1,22} Mounting evidence now suggests that axillary clearance can be safely omitted in certain cases if the metastasis is smaller than 2 mm (isolated tumour cells/micro-metastasis) or macro-metastases of no more than two lymph nodes in the SLNs.^{23,24} Maguire and Brogi have recently highlighted the fact that the primary purpose of examining SLNs is to identify all macro-metastases (>2 mm).²⁰ This poses a new challenge for the current methods of intraoperative SLN diagnosis, which must be fast and accurate²⁵ while ensuring precise measurement. Herein, we have proposed the use of a modified MEW-M system with high feasibility and diagnostic efficiency, to facilitate intraoperative SLN status assessment in these scenarios.

MEW-M is a novel portable imaging microscopy technique that generates real-time and non-destructive pseudo-histological images of tissue. The main advantage of this device is its optimised image stabilisation (OIS) anti-shaking design and frame rate of up to 60 frames/s, ensuring real-time histomorphological feedback while scanning tissue. In addition, with an ultra-high-resolution lens, the morphology and arrangement of the cells are clearly visible on the monitor. Our preclinical study found that the imaging capability of MEW-M was highly consistent with that of H&E, providing a close match in terms of both spatial resolution and the ability to recognise the structural organisation of a sample. Additionally, the image quality scores, according to a junior pathologist, indicated that MEW-M had superior image quality than TIC, with a median score of 3.1 vs 2.1 ($p < 0.0001$). Furthermore, the lower cellular content and incomplete pathological structure in TIC made interpretation more challenging, such that a dedicated pathologist was required to resolve the issue.²⁶ From this perspective, promoting the use of MEW-M in clinical settings could prove beneficial.

Diagnostic accuracy is the primary concern when evaluating the merits of new technologies.²⁷ Likelihood ratios (LR) were used here as an alternative statistic for summarising diagnostic accuracy, as this approach does not depend on disease prevalence and is a more clinically useful measure than sensitivity and specificity.²⁸ LR was divided into PLR and NLR, where PLR is the ratio of the probability of a specific test result in a diseased population to the probability in a non-diseased population,²⁹ and NLR is the opposite.³⁰ Typically a PLR above 10/NLR value below 0.1 would be considered strong evidence with which to rule in/rule out disease.³¹ Moreover, the farther

a PLR value is from 1, the stronger the evidence for the presence of the disease, and vice versa for NLR. Our results show that the two methods are highly accurate in the assessment of SLN status. Both PLR values were well above 10, and the NLR values were below 0.1, indicating that both methods exhibited excellent performance. However, our TIC figures are somewhat inconsistent with those of several studies that have larger sample sizes, especially in the observed differences in NLR values (0.174–0.429).^{6,32} In addition, our previous report also indicated poor NLR in TIC, with a value of 0.33, yielding a miss rate of 35%.³³ Horváth et al reported an excessive false positive rate of TIC from their centre; according to the updated guidelines, 15.32% of the resulting axillary clearances were unnecessary.⁶ These discrepancies arise mainly due to the lack of recognition of micro-metastases by TIC as well as the heterogeneity between groups in the proportion of micro-metastases, which accounted for a high proportion of positive groups in their cohort (21.2%, compared to only 5.5% in our cohort). The poor recognition of micro-metastases (0/3) by TIC in our study is consistent with the findings reported in the literature.^{6,7,34} Despite this limitation, in the context of model 2, there remains no statistically significant difference in diagnostic efficacy between MEW-M and TIC. However, MEW-M has demonstrated strong discriminatory power in the detection of macro-metastasis, and the deposit size can be easily calculated by superimposing the microscopic FOV. Lastly, the integrated analysis also supported the view that MEW-M is 100% accurate for positive event judgements, with an infinitely great PLR value in model 2. Bharath et al have recently published a systematic review and meta-analysis of TIC and frozen section biopsy and their comparison for the evaluation of SLNs in breast cancer.⁷ Their data showed that the pooled specificity of TIC was 98%.⁷ In addition, Saeed et al have recently reported a prospective study for the evaluation of intraoperative TIC of SLN in comparison to permanent histology diagnoses in 25 breast cancer patients.³⁵ Their results showed that TIC has high specificity, with a 6.25% false positive rate.³⁵ Furthermore, Uno et al conducted a retrospective cytology-histology correlation study to evaluate the value and practical utility of intraoperative TIC of SLN in patients with breast cancer.³⁶ Their results also showed that TIC has a specificity value of 100%.³⁶ Admittedly, TIC remains a useful method with relatively high sensitivity, specificity, and accuracy and therefore can be used as a rapid and economical test. It can be used as a substitute for MEW-M, particularly in low-resource settings, as MEW-M is relatively expensive compared to TIC. However, MEW-M is simpler and faster, and, unlike TIC, does not require the involvement of pathologists, thus enabling savings in terms of human resources.

The timeliness of the intraoperative result is another issue of concern to surgeons.²⁵ Though reports have shown that it is currently the fastest technique in a clinical setting, Hadalin et al cast doubt on the time-consuming nature of TIC's intraoperative feedback.³⁷ We observed a considerable speed advantage of MEW-M in our work, reducing reporting time by 9 minutes per session compared to TIC, with a median value of 10.3 min (range: 4–20 min) vs 19.4 min (range: 10–31 min). Generally, MEW-M and TIC feedback can be obtained in

4 min and 10 min, respectively, for patients with only 1 SLN, plus approximately 2 min (MEW-M) and 3 min (TIC) extra for an additional node. One of the defining features of MEW-M interpretation is that we uniformly stain specimens and greatly shorten the duration of the reporting process during scanning and interpretation. Our results show that MEW-M can easily be carried out within a limited time frame without delaying the operation.

The major limitation of the present study is data bias. The proportion of micro-metastatic cases was too small to accurately reflect the difference in diagnostic accuracy between the two techniques, especially for the model 2 analysis. As the sample size of micro-metastatic cases increases, we believe that the accuracy of MEW-M in model 2 will be shown to be superior to that of TIC. However, a detection rate of up to 35% for micro-metastasis³⁸ will lead to an increase in the number of false positives in model 2, which would adversely affect the NLR performance. In addition, the high diagnostic accuracy of TIC may not represent the average level in China, since TIC has been routinely used for more than 15 years at our institute. As mentioned above, MEW-M has several advantages: it is simpler, faster, and does not require the involvement of dedicated pathologists and may therefore address the shortage of human resources in pathology departments worldwide. Another weakness of the study is the lack of the whole digitised images of the cases assessed by MEW-M, which means that other pathologists are not able to fully review the tissue sample. We hope that this product can be improved further. Lastly, additional comparisons of the difficulty of MEW-M interpretation by pathologists with different levels of experience are warranted, even though we have assessed image quality and image characteristics here. Further research should be undertaken to explore larger, multi-centre trials and generate more convincing evidence in favour of the adoption of this approach.

5 | CONCLUSIONS

MEW-M is a promising technique that can be utilised to provide a rapid and accurate intraoperative assessment of SLN in a clinical setting to help improve decision-making in axillary surgery.

AUTHOR CONTRIBUTIONS

The authors' contributions to this study and the preparation of the manuscript are as follows. Jia-jian Chen and Jiong Wu designed the research. Jia-jian Chen, Shuang Hao, Ti-jing Shen, and Ying Wang performed the surgeries. Bao-hua Yu, Li-rui Yang, and Wen-tao Yang provided the final pathology results. Fei Ren provided the intraoperative touch imprint cytology results. Yuan Dong and Ming-jie Zheng evaluated the specimens with the MEW-M system. Jia-jian Chen conducted the statistical analysis and wrote the manuscript. The study protocol is available from the corresponding author.

ACKNOWLEDGEMENTS

The MEW-M system was provided by Dendrite Precision Instruments Inc., who also provided essential engineering, operational and

interpretation assistance without financial aid. It is important to note that no funding was received to support this study.

CONFLICT OF INTEREST STATEMENT

The EndoScell system was provided by Dendrite Precision Instruments Inc., who also provided important engineering, operational and interpretation assistance. Fudan University Shanghai Cancer Center has no financial or marketing relationship with Dendrite Precision Instruments Inc. for the technology described above. The authors declare no financial or marketing relationship with Dendrite Precision Instruments Inc. for the technology described above.

DATA AVAILABILITY STATEMENT

The data that supports the findings of this study are available in the Supporting Information that accompanies this article, and the complete images and videos are available from the corresponding author and first author.

ORCID

Jia-jian Chen  <https://orcid.org/0000-0001-9202-404X>

REFERENCES

- Laws A, Kantor O, King TA. Surgical management of the axilla for breast cancer. *Hematol Oncol Clin North Am*. 2023;37(1):51-77. doi:10.1016/j.hoc.2022.08.005
- Magnoni F, Galimberti V, Corso G, Intra M, Sacchini V, Veronesi P. Axillary surgery in breast cancer: an updated historical perspective. *Semin Oncol*. 2020;47(6):341-352. doi:10.1053/j.seminoncol.2020.09.001
- Ditsch N, Wöcke A, Untch M, et al. AGO recommendations for the diagnosis and treatment of patients with early breast cancer: update 2022. *Breast Care (Basel Switz)*. 2022;17(4):403-420. doi:10.1159/000524879
- Gradishar WJ, Moran MS, Abraham J, et al. Breast cancer, version 3.2022, NCCN clinical practice guidelines in oncology. *J Natl Compr Canc Netw*. 2022;20(6):691-722. doi:10.6004/jnccn.2022.0030
- Miltenburg DM, Miller C, Karamlou TB, Brunicardi FC. Meta-analysis of sentinel lymph node biopsy in breast cancer. *J Surg Res*. 1999;84(2):138-142.
- Horváth Z, Paszt A, Simonka Z, et al. Is intraoperative touch imprint cytology indicated in the surgical treatment of early breast cancers? *Eur J Surg Oncol EJSO*. 2017;43(7):1252-1257. doi:10.1016/j.ejso.2017.01.003
- Bharath S, Sharma D, Yadav SK, Shekhar S, Jha CK. A systematic review and meta-analysis of touch imprint cytology and frozen section biopsy and their comparison for evaluation of sentinel lymph node in breast cancer. *World J Surg*. 2022;47(2):478-488. doi:10.1007/s00268-022-06800-w
- Abe M, Yamada T, Nakano A. Prospective comparison of intraoperative touch imprint cytology and frozen section histology on axillary sentinel lymph nodes in early breast cancer patients. *Acta Cytol*. 2020;64(5):492-497. doi:10.1159/000508016
- Sai-Giridhar P, Al-Ramadhani S, George D, et al. A multicentre validation of Metasin: a molecular assay for the intraoperative assessment of sentinel lymph nodes from breast cancer patients. *Histopathology*. 2016;68(6):875-887. doi:10.1111/his.12863
- Voskuil FJ, Vonk J, van der Vegt B, et al. Intraoperative imaging in pathology-assisted surgery. *Nat Biomed Eng*. 2022;6(5):503-514. doi:10.1038/s41551-021-00808-8
- Nguyen FT, Zysk AM, Chaney EJ, et al. Intraoperative evaluation of breast tumor margins with optical coherence tomography. *Cancer Res*. 2009;69(22):8790-8796. doi:10.1158/0008-5472.CAN-08-4340
- Pekmezci M, Morshed RA, Chunduru P, et al. Detection of glioma infiltration at the tumor margin using quantitative stimulated Raman scattering histology. *Sci Rep*. 2021;11(1):12162. doi:10.1038/s41598-021-91648-8
- Menes TS, Tartter PI, Mizrahi H, Smith SR, Estabrook A. Touch preparation or frozen section for intraoperative detection of sentinel lymph node metastases from breast cancer. *Ann Surg Oncol*. 2003;10(10):1166-1170.
- Tew K, Irwig L, Matthews A, Crowe P, Macaskill P. Meta-analysis of sentinel node imprint cytology in breast cancer. *Br J Surg*. 2005;92(9):1068-1080. doi:10.1002/bjs.5139
- D'Halluin F, Tas P, Rouquette S, et al. Intra-operative touch preparation cytology following lumpectomy for breast cancer: a series of 400 procedures. *The Breast*. 2009;18(4):248-253. doi:10.1016/j.breast.2009.05.002
- Compton ML, Sweeting RS, Reisenbichler ES. Intraoperative sentinel lymph node evaluation: optimizing surgical pathology practices in an era of changing clinical management. *Ann Diagn Pathol*. 2018;33:45-50. doi:10.1016/j.anndiagpath.2017.12.003
- Zhang Y, Xie M, Xue R, et al. A novel cell morphology analyzer application in head and neck cancer. *Int J Gen Med*. 2021;14:9307-9313. doi:10.2147/IJGM.S341420
- Chen YW, Lin JS, Wu CH, Lui MT, Kao SY, Fong Y. Application of vivo stain of methylene blue as a diagnostic aid in the early detection and screening of oral squamous cell carcinoma and precancerous lesions. *J Chin Med Assoc*. 2007;70(11):497-503.
- Somasundaram SK, Chicken DW, Waddington WA, Bomanji J, PJ, Keshtgar MRS. Sentinel node imaging in breast cancer using superficial injections: technical details and observations. *Eur J Surg Oncol*. 2009;35(12):1250-1256. doi:10.1016/j.ejso.2009.05.006
- Maguire A, Brogi E. Sentinel lymph nodes for breast carcinoma: a paradigm shift. *Arch Pathol Lab Med*. 2016;140(8):791-795. doi:10.5858/arpa.2015-0140-RA
- Negida A, Fahim NK, Negida Y. Sample size calculation guide—part 4: how to calculate the sample size for a diagnostic test accuracy study based on sensitivity, specificity, and the area under the ROC curve. *Adv J Emerg Med*. 2019;3(3):e33. doi:10.22114/ajem.v0i0.158
- Brackstone M, Baldassarre FG, Perera FE, et al. Management of the axilla in early-stage breast cancer: Ontario Health (Cancer Care Ontario) and ASCO guideline. *J Clin Oncol*. 2021;39(27):3056-3082. doi:10.1200/JCO.21.00934
- Krag DN, Anderson SJ, Julian TB, et al. Sentinel-lymph-node resection compared with conventional axillary-lymph-node dissection in clinically node-negative patients with breast cancer: overall survival findings from the NSABP B-32 randomised phase 3 trial. *Lancet Oncol*. 2010;11(10):927-933. doi:10.1016/S1470-2045(10)70207-2
- Donker M, van Tienhoven G, Straver ME, et al. Radiotherapy or surgery of the axilla after a positive sentinel node in breast cancer (EORTC 10981-22023 AMAROS): a randomised, multicentre, open-label, phase 3 non-inferiority trial. *Lancet Oncol*. 2014;15(12):1303-1310. doi:10.1016/S1470-2045(14)70460-7
- Nolan RM, Adie SG, Marjanovic M, et al. Intraoperative optical coherence tomography for assessing human lymph nodes for metastatic cancer. *BMC Cancer*. 2016;16(1):144. doi:10.1186/s12885-016-2194-4
- Mohammadnia Avval M, Hosseinzadeh M, Farahi Z, Mirtalebi M. Comparing scraping cytology with touch imprint cytology and frozen section analysis in the intraoperative diagnosis of sentinel lymph node metastasis in breast cancer. *Diagn Cytopathol*. 2021;49(4):475-479. doi:10.1002/dc.24695

27. Yang H, Zhang S, Liu P, et al. Use of high-resolution full-field optical coherence tomography and dynamic cell imaging for rapid intraoperative diagnosis during breast cancer surgery. *Cancer*. 2020;126(Suppl 16):3847-3856. doi:10.1002/cncr.32838
28. Diagnostic EP. Accuracy measures. *Cerebrovasc Dis*. 2013;36(4):267-272. doi:10.1159/000353863
29. Tatekawa H, Uetani H, Hagiwara A, et al. Worse prognosis for IDH wild-type diffuse gliomas with larger residual biological tumor burden. *Ann Nucl Med*. 2021;35(9):1022-1029. doi:10.1007/s12149-021-01637-0
30. Deeks JJ, Altman DG. Diagnostic tests 4: likelihood ratios. *BMJ*. 2004;329:168-169. doi:10.1136/bmj.329.7458.168
31. Yaroslavsky AN, Feng X, Muzikansky A, Hamblin MR. Fluorescence polarization of methylene blue as a quantitative marker of breast cancer at the cellular level. *Sci Rep*. 2019;9(1):940. doi:10.1038/s41598-018-38265-0
32. Chang YC, Tzen CY. Intraoperative sentinel lymph node imprint cytology diagnosis in breast cancer patients by general surgical pathologists: a single-institution experience of 4327 cases. *J Cytol*. 2022;39(1):20-25. doi:10.4103/JOC.JOC_41_21
33. Jia-jian C, Ben-long Y, Jia-ying C, et al. A prospective comparison of molecular assay and touch imprint cytology for intraoperative evaluation of sentinel lymph nodes. *Chin Med J (Engl)*. 2011;124(4):491-497.
34. Fujishima M, Watatani M, Inui H, et al. Touch imprint cytology with cytokeratin immunostaining versus Papanicolaou staining for intraoperative evaluation of sentinel lymph node metastasis in clinically node-negative breast cancer. *Eur J Surg Oncol*. 2009;35(4):398-402. doi:10.1016/j.ejso.2008.03.004
35. Saeed MS, Al-Lawati T, Lawati FA, Elias RN. Evaluation of intraoperative touch imprint cytology of axillary sentinel lymph node accuracy in comparison to the permanent histology diagnosis. a prospective study of 25 invasive breast cancers. *Gulf J Oncol*. 2021;1(37):70-78.
36. Uno Y, Akiyama N, Yuzawa S, Kitada M, Takei H. The value and practical utility of intraoperative touch imprint cytology of sentinel lymph node(s) in patients with breast cancer: a retrospective cytology-histology correlation study. *Cytojournal*. 2020;17:11. doi:10.25259/Cytojournal_80_2019
37. Hadalin V, Pislari N, Borstnar S, et al. Intraoperative touch imprint cytology in breast cancer patients after neoadjuvant chemotherapy. *Clin Breast Cancer*. 2022;22(4):e597-e603. doi:10.1016/j.clbc.2021.12.013
38. Pétursson HI, Kovács A, Mattsson J, Olofsson BR. Evaluation of intraoperative touch imprint cytology on axillary sentinel lymph nodes in invasive breast carcinomas, a retrospective study of 1227 patients comparing sensitivity in the different tumor subtypes. *PLoS ONE*. 2018;13(4):e0195560. doi:10.1371/journal.pone.0195560

SUPPORTING INFORMATION

Additional supporting information can be found online in the Supporting Information section at the end of this article.

How to cite this article: Chen J-j, Yu B-h, Shen T-j, et al. A prospective comparison of a modified miniaturised hand-held epifluorescence microscope and touch imprint cytology for evaluation of axillary sentinel lymph nodes intraoperatively in breast cancer patients. *Cytopathology*. 2023;00:1-9. doi:10.1111/cyt.13312